Journal of Non-Crystalline Solids 356 (2010) 1325–1331

Contents lists available at ScienceDirect

Journal of Non-Crystalline Solids

journal homepage: www.elsevier.com/ locate/ jnoncrysol

Structure and mechanical properties of silica aerogels and xerogels modeled by molecular dynamics simulation

John S. Rivas Murillo [a,*], Martina E. Bachlechner [b], Fritz A. Campo [a], Ever J. Barbero [a]

[a] Mechanical and Aerospace Engineering Department, West Virgina University, Morgantown, WV 26506, United States
[b] Computer Science, Math and Physics Department, Fairmont State University, Fairmont, WV 26554, United States

ARTICLE INFO

Article history:
Received 21 May 2009
Received in revised form 29 January 2010
Available online 14 May 2010

Keywords:
Aerogels;
Fractals;
Mechanical properties;
Molecular dynamics;
Simulations

ABSTRACT

In this article a study of the structural and mechanical properties of porous silica is presented. The procedure to prepare the samples consists in expanding single crystals of β-cristobalite to reach the desired density followed by a thermal treatment. The resulting porous structures have densities in the range from 0.23 to 2.2 g/cm^3. The structure of the samples is studied by obtaining the fractal dimension using two different methods, one based on the pair distribution function and the other one based on the simulation of a scattering experiment. The values of the fractal dimension were found to be in good agreement with previously published data from experiments and comparable computer simulations. The mechanical properties, namely elastic modulus and strength, are studied through the simulation of a tension test. The elastic modulus and the strength relate to density by a power law characterized by exponents of 3.11 ± 0.21 and 2.53 ± 0.15 respectively. A comparison of that data to previously published data is included. The results proved that the direct expansion, coupled with thermal processing of the sample, leads to systems suitable to investigate the structure and the mechanical properties of silica aerogels.

1. Introduction

Aerogels and xerogels are nanoporous materials with interesting properties from both scientific and industrial points of view. They can be produced using any material, provided that it can form multifunctional monomers that cross-link forming a gel, and that such a gel can undergo the process of venting the liquid out the solid face without causing its collapse [1]. In the case of silica aerogels and xerogels, some of the properties that characterize them are their very low density, as low as 0.003 g/cm^3 which is only three times greater than that of air, surface area as large as 1000 m^2/g, a refraction index only 5% greater than that of air, the lowest thermal conductivity among all solid materials, a speed of sound approximately three times smaller than that of air, and a dielectric constant only 10% greater than that of vacuum. Those properties make aerogels and xerogels attractive materials for applications such as catalysts, fuel cells, high performance windows, supercapacitors, heat barriers, particle traps, ultrasound probes, and ion exchange media [1–4].

Experimentally, aerogels and xerogels are made by sol–gel processing. The processing starts with the hydrolysis of a silica precursor, typically tetramethyl ortho silane (TMOS, $Si(OCH_3)_4$) or tetraethyl ortho silane (TEOS, $Si(xOC_2H_5)_4$); however other precursors can be used, too. For example, Steven Kistler, who is considered to have discovered this type of materials [1], produced the first silica aerogel using sodium silicate (Na_2SiO_3) dissolved in a solution of hydrochloridric acid (HCl) and water [2]. The pH of the solution can be controlled by adding acidic or basic additives; those will react with neither the silica precursor nor the water but will affect the rate at which the hydrolysis proceeds as well as the final structure of the porous solid [5–7].

After the hydrolysis, polycondensation of silica occurs and the solution becomes a gel. A large change of the viscosity indicates the gelation of the solution. At this point a nanoporous solid skeleton of silica is formed inside the solution and fills almost all its volume. If the gel is dried at room temperature and atmospheric pressure, large shrinkage of the solid structure is caused along with large reduction of the porosity. The shrinkage is mainly due to the stresses exerted on the solid branches when the liquid evaporates. Materials obtained this way are called xerogels and have porosities as high as 50%, corresponding to a density of 1.1 g/cm^3. To avoid excessive shrinkage, the pressure and the temperature of the gel are increased until the critical point of the liquid phase has been exceeded. Under those conditions there is no liquid/vapor interface and no surface tension. Therefore, no large stresses are exerted on the solid skeleton and the shrinkage is highly reduced. Solids processed at supercritical conditions reach porosities up to 99.8% and are called aerogels [2].

Although the internal structure of aerogels and xerogels is responsible for their outstanding properties, such as large surface area and low thermal conductivity, it is also responsible for its relatively poor mechanical response. The tensile strength and the elastic modulus of aerogels and xerogels can be up to four orders of magnitude smaller

* Corresponding author.
E-mail address: jrivasmu@mix.wvu.edu (J.S. Rivas Murillo).

0022-3093/$ – see front matter © 2010 Elsevier B.V. All rights reserved.
doi:10.1016/j.jnoncrysol.2010.03.019

than those of dense silica glass, as it is confirmed by three-point bending and diametral compression tests done by Woignier et al. [7–9], and studies made by Groß et al. [10] using the ultrasonic pulsed-echo method. It is important to study the mechanical properties of this type of material, in particular aerogels, because their poor mechanical response limits their usage. For instance, the production of crack-free monolithic tiles becomes difficult due to the brittleness of the material [11] which affects its application in glazing systems where cracks are associated with light scattering [12,13]. Also the use of aerogels as reaction platforms requires very delicate handling, and their weakness limits the usefulness of the material in this context [14].

Studies of the structure and properties of aerogels and xerogels are done via experiments and computer simulations. Experimentally, using small angle neutron scattering (SANS) and nuclear magnetic resonance (NMR), it has been observed that aerogels and xerogels are fractal structures characterized by a fractal dimension varying from 3 for very low porosity (almost dense glass) to 1.8 for very light specimens. The fractal dimension is slightly affected by the pH of the solution prior to gelation [7,15–17]. Vacher et al. [15] found through SANS that aerogel samples with densities smaller than 0.43 g/cm^3 prepared under acidic and neutral conditions have a fractal dimension around 2.4 ± 0.03. A fractal dimension of 2.2 was found by Devreux et al. [16] for aerogels with densities around 0.17 g/cm^3 prepared under acidic conditions. Confirmation of those results is provided by Woignier et al. [7,17], who studied aerogels prepared under acidic, basic and neutral pH finding that under basic conditions aerogels have a fractal dimension close to 1.8 ± 0.1, while under acidic or neutral conditions the samples had a fractal dimension around 2.2 ± 0.1 and 2.4 ± 0.1 respectively.

In computational research, Molecular Dynamics (MD) simulations are used in Kieffer and Angell and Nakano et al. [18,19] to generate surrogate (computer models) of silica aerogels. Kieffer and Angell [18] propose to use MD to model silica aerogel and xerogel starting from a sample of silica glass that is gradually expanded. The expansion causes breaking of the Si–O bonds and leads to the formation of a fractal structure characterized by a fractal dimension that changes linearly with density. However the linearity is not sustained for samples with densities higher than 1 g/cm^3. Kieffer and Angell [18] use an interaction potential of the Born–Mayer form, which accounts for two-body interactions, to model a system containing between 300 and 1500 particles.

Nakano et al. [19] use a potential including two-body and three-body interaction components to model porous silica with densities varying from 2.2 g/cm^3 to 0.2 g/cm^3 in a system composed of 41,472 particles. Similar to Kieffer and Angell [18], Nakano et al. [19] gradually expand the system until the desired density is reached and investigate the dependence of the fractal dimension, internal surface area, the pore to volume ratio, pore size distribution, correlation length, and mean particle size on the density of the sample.

Campbell et al. [20], using the same potential as Nakano et al. [19], generate porous samples by placing spherical clusters of dense silica glass in a large volume and sintering the system at constant pressure and temperature. With that approach they generate samples of densities varying from 1.67 g/cm^3 to 2.2 g/cm^3, a range of density corresponding to xerogels, and study the changes on the short-range and intermediate-range order of the structure with density. They also study the effect of densification on the elastic modulus of the samples, finding a power law relation between modulus and density with an exponent of 3.5 ± 0.2.

In the present study the potential used by Nakano et al. [19] is adopted, however a different approach to prepare the samples is proposed. The volume of a dense crystalline sample (β-cristobalite) is expanded in one step to the desired density. Then the temperature is increased to give the atoms enough energy to diffuse through the system, and finally it is cooled down in a stepwise process. This process resembles a diffusion limited aggregation [18]. Since the atoms are initially set at distances larger than their equilibrium distances and have high kinetic energy, they can diffuse to farther regions in the simulation volume and could potentially form any kind of structure. That is an advantage of this procedure over the gradual expansion, where the atoms can only move short distances and are bounded to remain in the same region. For this study samples with densities varying from 0.23 g/cm^3 to 2.2 g/cm^3 (dense glass) are produced. The fractal dimensions for those samples are calculated based on the decay of the pair distribution functions (PDF) and simulated scattering experiments. The results obtained in this study, geometrical and mechanical properties of porous silica, are in the ranges found experimentally.

The interatomic potential chosen for this study was developed by Vashishta et al. [21,22]. It is used because it accurately reproduces the structural parameters for dense silica glass. Using the factor R_χ introduced by Wright [23] to compare the experimental results of neutron scattering with computer simulations this potential produces an error of only 4.4%, which is the smallest among all the available potentials for silica [20]. Vashishta's potential also excels in the representation of the elasticity of silica glass. The elastic modulus of glass calculated using this potential has been reported to be around 70 GPa [20], which compares well to the experimental value of 71.9 GPa reported by Muralidharan et al. [24].

The MD simulation procedure used to prepare the aerogel and xerogel samples is introduced first. Next, methods for obtaining the fractal dimension and the mechanical properties of the samples are described. Then the characteristics of the samples, the fractal dimension, elastic modulus, and strength are discussed in relation to density.

2. Aerogel and xerogel simulation

2.1. Interatomic potential

The interatomic potential is the key component of any MD simulation. It represents the most important interactions among atoms, i.e. bonding interactions, interactions with non-bonding neighbors, and the extension of those interactions. If the interatomic potential does not accurately describe the interactomic interactions, the simulation results will not be representative of the actual material.

The interatomic potential used for this study is the one developed by Vashishta et al. [21,22] for amorphous silica. It involves terms representing the interaction between two atoms (two-body component); which, disregarding if the atoms bond or not, accounts for the potential energy due to the distance between them. The potential also includes the potential energy due to the change of orientation and bonding angle of triplets of atoms (three-body component). The two-body and three-body components of the potential are given by

$$V_{ij}^{(2)} = \frac{H_{ij}}{r_{ij}^{\eta_{ij}}} + \frac{Z_i Z_j}{r_{ij}} \exp\left(\frac{-r_{ij}}{r_{1s}}\right) - \frac{P_{ij}}{r_{ij}^4} \exp\left(\frac{-r_{ij}}{r_{4s}}\right) \quad (1)$$

$$V_{jik}^{(3)} = B_{jik} f\left(r_{ij}, r_{ik}\right)\left(\cos\theta_{jik} - \cos\tilde{\theta}_{jik}\right)^2 \quad (2)$$

In the previous equations r_{ij} is the distance between the atoms i and j. The first term of Eq. (1) represents the steric repulsion due to the atomic size. The parameters H_{ij} and η_{ij} are the strength and exponent of steric repulsion. The second term corresponds to the Coulomb interactions between the atoms and accounts for the electric charge transfer, where Z_i is the effective charge of the ith ion. The third term includes the charge–dipole interactions. It takes into account the electric polarizability of the atoms through the variable P_{ij}, which is given by $P_{ij} = \frac{1}{2}\left(\alpha_i Z_j^2 + \alpha_j Z_i^2\right)$; where α_i is the electric polarizability of the ith ion. The parameters r_{1s} and r_{4s} are cut-off values for the interactions.

In Eq. (2), B_{jik} is the strength of the three-body interaction, θ_{jik} is the angle between the vector position of the atoms, i.e. r_{ij} and r_{ik}. The function f represents the effect of bond stretching and the component containing ($\cos\theta_{jik}$) takes into account the bending of the bonds,

and θ_{jik} is a reference angle for the respective interaction. Although, there are six possible three-body interactions in the system, this potential only considers the most dominant ones, which are related to (Si–O–Si) and (O–Si–O) angles. More information about the potential, including the values of the parameters, is available in Refs. [21,22].

2.2. Sample preparation

The simulations done to generate and characterize the samples of silica aerogel and xerogel considered for this study were performed using an in-house fortran program, which has been used successfully to investigate structural and mechanical properties of silicon nitrate [25] and silicon carbide [26] systems. In this code the Velocity–Verlet algorithm is used to solve the equations of motion of the particles, using a time step of 0.5 fs. Langevin dynamics is implemented and all the particles in the system are used to control its temperature accordingly.

The procedure to generate the porous samples analyzed in this study follows the steps listed below:

i. Placing the atoms at the crystalline sites of β-cristobalite with a lattice constant corresponding to the desired density.
ii. Heating up of the system to 3000 K.
iii. Cooling down of the system allowing relaxation at several temperatures.

β-cristoballite is selected as starting material because it has the same density as silica glass (2.2 g/cm^3). The atomic coordinates for β-cristoballite are given by Wyckoff [27]. The goal of this process is to create a uniform distribution of atoms across the volume. The expanded samples are heated up to 3000 K and held at that temperature for about 50 ps. Keeping the system at high temperature, along with the cooling scheme, eliminates the effect of the initial positions of the atoms.

The complete thermal treatment involves heating the sample under controlled temperature conditions for about 30 ps, then the temperature control is removed and the samples are relaxed. For cooling the samples the same strategy of temperature control and relaxation is used. During cooling, the systems are relaxed at 2500, 2000, 1500, 600, 300, and 0 K to allow diffusion of the atoms. For the simulations presented here periodic boundary conditions and a time step equal to 0.5 fs are used. The selection of a small time step ensures that the atoms do not fly off, which is important in this case because large free surfaces are generated inside the samples.

The crystalline samples used have a size of about 71^3 Å^3 containing 24,000 atoms. They are expanded to obtain eight different systems with volumes of 81^3, 91^3, 101^3, 111^3, 121^3, 131^3, 141^3, and 151^3 Å^3, and having densities of about 1.48, 1.05, 0.77, 0.58, 0.45, 0.35, 0.28, and 0.23 g/cm^3 respectively.

2.3. Geometrical characterization

Once MD has been used to generate the samples, the fractal dimension can be obtained based on its relation to the pair distribution function (PDF) of the samples. The PDF represents the probability of finding a pair of atoms separated by a distance r in the structure, relative to the probability expected for a randomly distributed structure having the same density [28]. The PDF is calculated as

$$g_{\alpha\beta}(r_1,r_2) = \frac{V^2}{N_\alpha N_\beta}\left\langle \sum_{i\in\{\alpha\}}^{N_\alpha}\sum_{j\in\{\beta\}}^{N_\beta}\delta(r_1-r_i)\delta\left(r_2-r_j\right)\right\rangle \tag{3}$$
$$= \rho_\alpha^{-1}\rho_\beta^{-1}\left\langle \sum_{i\in\{\alpha\}}^{N_\alpha}\sum_{j\in\{\beta\}}^{N_\beta}\delta(r_1-r_i)\delta\left(r_2-r_j\right)\right\rangle$$

where V is the volume of the system, N_α and N_β are the numbers of particles of the entities of type α and β respectively, ρ_α and ρ_β are the corresponding densities of α and β subsystems, and the symbol $\langle\rangle$ means ensemble average. Therefore, several configurations of the system should be used to compute the PDF. The term inside the $\langle\rangle$ symbol indicates that when finding the distribution of distances between the atoms of type α and β one must locate each atom of type α and obtain the distance from it to each one of the atoms of type β.

An example of the PDF for one of the systems created in this study is shown in Fig. 1. In the inset of Fig. 1 the decay of the PDF for large values of the distance between the atoms is shown. That decay can be used to estimate the fractal dimension, d_f, of porous systems [18] by using the relation:

$$d_f = 3 + \frac{d\mathrm{Log}(g(r))}{d\mathrm{Log}(r)} \tag{4}$$

Another way of obtaining the fractal dimension of a structure is through a simulated scattering experiment [29,30]. To simulate a scattering experiment one needs to calculate the scattering intensity, I, corresponding to different wavelengths of radiation shined to the sample, represented by their wave number, q. An expression to calculate I, when the positions of all the particles in the system are know, is given by [31,32]:

$$\frac{I(q)}{I_0} = \sum_{ij}\frac{\sin\left(qr_{ij}\right)}{qr_{ij}} \tag{5}$$

where I is the scattering intensity, I_0 is a reference value of intensity, q is the wave number and r_{ij} is the distance between two atoms i and j.

For fractal structures, the scattering intensity can be related to the wave number by a power law, where the exponent is the negative of the fractal dimension of the structure, i.e. $I \propto q^{-df}$ [31,32]. An example of the $I(q)$ is plotted in the Fig. 2. For large wave numbers the scattering intensity corresponds to the individual particles and remains constant; while for small wave numbers, clusters of particles are responsible for the scattering. The limiting value of wave number in the scattering is determined by the size of the sample modeled.

2.4. Mechanical characterization of the samples

A tension test is simulated by stretching the sample along one direction at a strain rate of 0.004 ps^{-1}. The strain rate is larger than the one used in laboratory tests; however it has been shown that smaller values of strain rate do not change the results significatively [33]. At higher strain rates, the speed of the atoms, and consequently the temperature of the sample, tend to increase. Nevertheless, if the stretching speed is not near the speed of sound in the material, the temperature can be controlled by selection of a proper thermostat [34]. In this study, Langevin dynamics [35] is used to control the speed

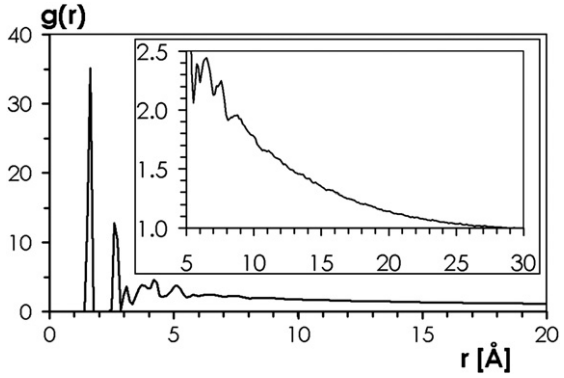

Fig. 1. Pair distribution function for a sample of density of 0.45 g/cm^3.

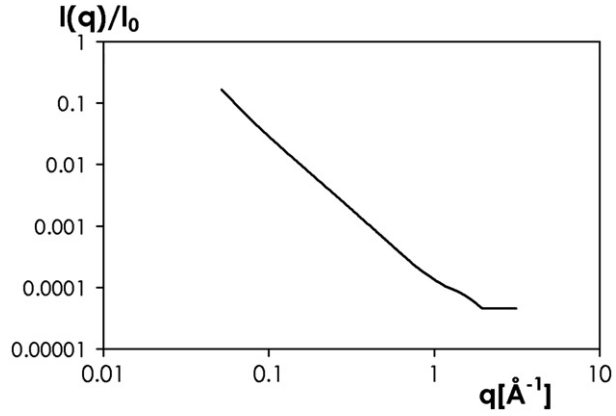

Fig. 2. Log–Log plot of the scattering intensity vs. wavenumber for a sample of density of 0.45 g/cm^3.

of all the atoms in the system. Langevin dynamics is based on the following equation,

$$m_i\ddot{\vec{r}}_i = \vec{F}_i - m_i\gamma_i\dot{\vec{r}}_i + \vec{R}_i(t) \quad (6)$$

where m_i is the mass of the atom, $\vec{r}_i$, $\dot{\vec{r}}_i$ and $\ddot{\vec{r}}_i$ are the position, velocity and acceleration of the particle, $\vec{F}_i$ is the force exerted on the particle by all the other particles in the system, $\vec{R}_i$ is a stochastic force applied to the particle, and γ_i is a damping coefficient. Previous studies on modeling bulk silica where used to select the combination of strain rate and the damping to use in the Langevin dynamics without affecting the results of the simulation [33].

3. Simulation results

3.1. Sample preparation

During the initial stages of the preparation process, and due to the high temperature of the system, the atoms have high kinetic energies, which allow them to move in groups formed by a small number of atoms. As the temperature of the system is reduced the number of atoms per group increases; but the atoms are still able to move in the system. Finally, when the temperature is low the atoms can only find equilibrium positions around their current locations, meaning that the structure has been locked. This preparation process is not intended to simulate the gelation process itself, but to allow the formation of samples resembling the structure of silica aerogels and xerogels, and responding to stimuli in a similar fashion that they do. How well this purpose is accomplished will be discussed in the Sections 2 and 3. At this point is important to remark that the simulated samples have branched structures formed by groups of atoms interconnected by small bridges.

Two of the samples generated for this study ($\rho = 0.58$ g/cm^3 and $\rho = 0.28$ g/cm^3) are shown in Fig. 3, where it can be observed that clusters interconnected by small chains are formed. Pores varying in size from a couple of atomic distances to several nanometers are thus obtained. Those pores have irregular shapes and can interconnect forming percolating paths inside the structure, which reflects the expected structure of silica aerogels very well.

3.2. Geometrical characterization

The pair distribution function of the samples produced for this study reflects that in the short-range order, features under 5 Å, the computational samples show characteristics similar to those of silica samples, namely a bonding distance (Si–O atoms) of 1.63 ± 0.03 Å, the nearest neighbors distances O to O atoms and Si to Si atoms are 2.65 ± 0.03 Å and 3.08 ± 0.03 Å, respectively. For experimental silica samples those quantities are 1.61 ± 0.05 Å for Si–O, 2.632 ± 0.089 Å for O–O, and 3.08 ± 0.10 Å for Si–Si [21].

In the range between 9 and 25 Å, approximately, the simulated samples exhibit a fractal behavior, which agrees with the fractal range found in simulations done by Nakano et al. [19], 5 to 25 Å. In aerogel samples studied by Vacher et al. tevacher88 the fractal range of the samples was identified extending from features as small as 4 Å to features larger than 200 Å, depending on the density of the sample. Courtens and Vacher [36] report that the fractal range of silica aerogels extends from 10 Å to 1000 Å, approximately.

The fractal dimension as a function of the density is plotted in Fig. 4. The values of fractal dimension from References [18,19], also shown in Fig. 4, were obtained using the PDF. As expected, the fractal dimension increases with the density toward a limiting value of 3, corresponding to bulk silica. For larger densities the scattering experiments lead to fractal dimensions slightly smaller than those obtained using the decay of the PDF. For lighter samples the opposite occurs.

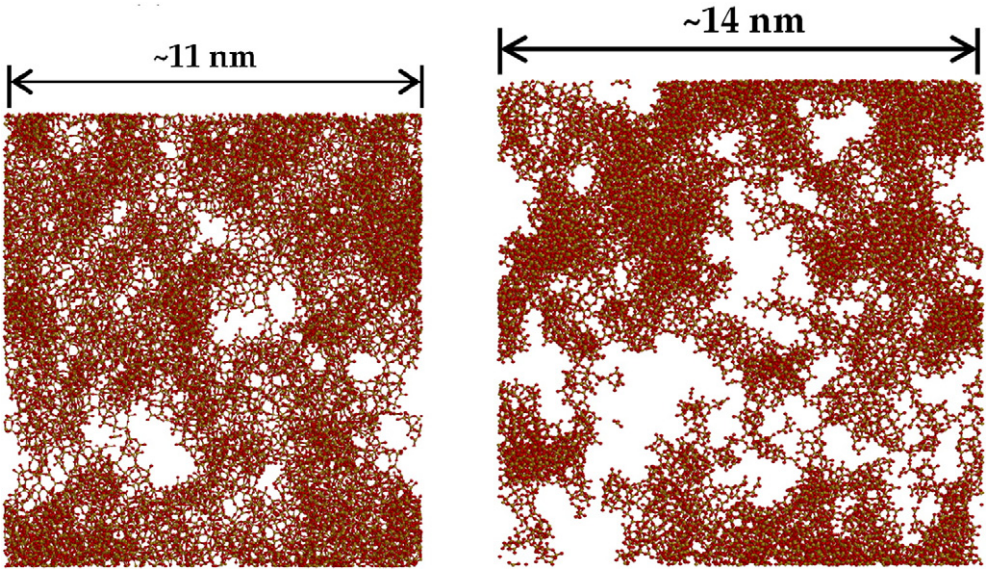

Fig. 3. Two samples generated for this study. Left: density of 0.58 g/cm^3, porosity of 74%. Right: density of 0.28 g/cm^3, porosity of 87%.

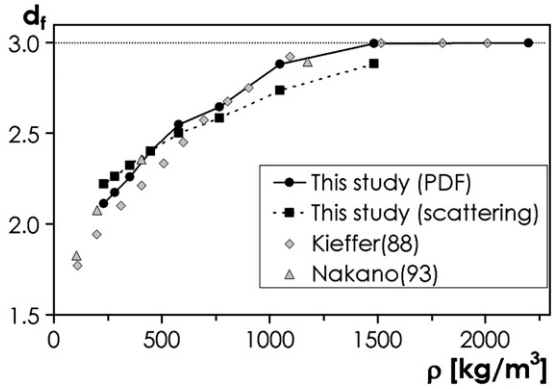

Fig. 4. Fractal dimension of silica aerogels samples with different densities.

The fractal dimension of the samples with densities in the range of aerogels is 2.33 ± 0.23. The value compares well with the value obtained by Courtens and Vacher [36], 2.40 ± 0.03, and by Woignier et al. citewoignier98, 2.2 ± 0.1 and 2.4 ± 0.1 for samples prepared under acid and neutral pH respectively.

3.3. Mechanical characterization

Data for the elastic moduli for different densities is presented in the Fig. 5 along with experimental data taken from Refs. [7] and [8]. The magnitude of the values obtained for the elastic modulus of the samples compares well with experimental data. Additionally, a power law can be used to describe the relation between it and density of the samples. From the results presented here the exponent for that relation is calculated as 3.11 ± 0.21. Comparison of that value and previously published data is summarized in Table 1. Although the exponent determined here differs from the one determined by Campbell et al. [20], it is important to notice that the range of densities modeled here is broader and the exponent lies in the range of the values found experimentally, from 2.97 to 3.8. The range of densities modeled in this research covers almost the same range that is covered by Woignier et al. [7] for partially densified samples (last row in Table 1). In that range our exponent, 3.11 ± 0.21, compares well to the one determined experimentally, 3.2 ± 0.2.

The relation between strength and density is plotted in the Fig. 6. It can be seen that a power law relation between strength and density exists. The exponent for that relation has been calculated as 2.53 ± 0.15, a value that compares well with previously published values summarized in Table 2. There is a difference between the magnitude of the strength from experiments and simulations. The value of the strength for dense glass obtained in this study was 4.4 GPa, which is four times smaller than the experimental value of 18 GPa reported in [24].

Table 1
Exponent for the power law relation between elastic modulus and density of porous silica.

Reference	Exponent	Density [g/cm^3]	Observations
This study	3.11 ± 0.21	0.23–2.2	Computer simulation
Campbell et al. [20]	3.5 ± 0.2	1.67–2.2	Computer simulation
Groß et al. [10]	3.49 ± 0.07	0.14–2.7	Exp.
Groß et al. [10]	2.97 ± 0.05	0.08–1.2	Exp. sintered aerogels
Woignier et al. [8]	3.8 ± 0.2	0.1–0.4 (approx. values)	Exp. pH neutral
Woignier et al. [7]	3.7 ± 0.2	0.055–0.5 (approx. values)	Exp. pH neutral, acidic and basic
Woignier et al. [7]	3.2 ± 0.2	0.42–2.2 (approx. values)	Exp. partially densified samples

4. Discussion

The preparation process of the computational samples leads to the formation of fractal structures resembling that of aerogels and xerogels. The short-range order features, i.e. interatomic distances, correspond to those of silica. The fractal features, although limited by the size of the samples, appear in the range expected for this type of materials (10–1000 Å). The value of the fractal dimension of the aerogels samples, 2.3 ± 0.23 compares well with experimental data obtained from samples processed under acid and neutral pH values. The fractal dimension tends to 3 (upper limit) as the density of the material tends to the bulk material. When the sample becomes lighter, near the percolation threshold, the lower limit for the fractal dimension is also satisfied.

Although the procedure used to generate the porous samples for this study does not correspond to the events happening during the experimental gelation of a solution, it produces samples having geometrical features that are similar to those of real aerogeland xerogel materials. For instance, they have the same type of relation between the fractal dimension and the density. This means that the direct expansion procedure coupled with the thermal treatment of the system increases the diffusivity of the atoms allowing them to reorganize and form fractal structures.

The structural analysis of the samples produced for this study is complemented by the mechanical characterization. The mechanical properties of the samples relate to density following a power law, which is typical of self-affine structures. Good agreement between the elasticity of the simulated samples and the experimental values from references is shown in Fig. 5. The elastic modulus for dense glass

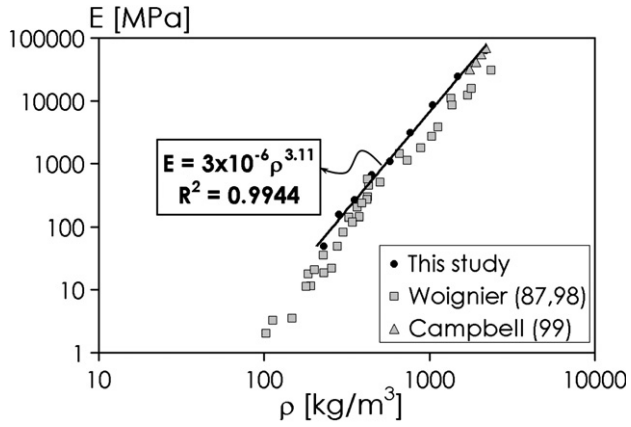

Fig. 5. Elastic modulus vs. density for silica aerogels. Campbell [20], Woignier [7,8].

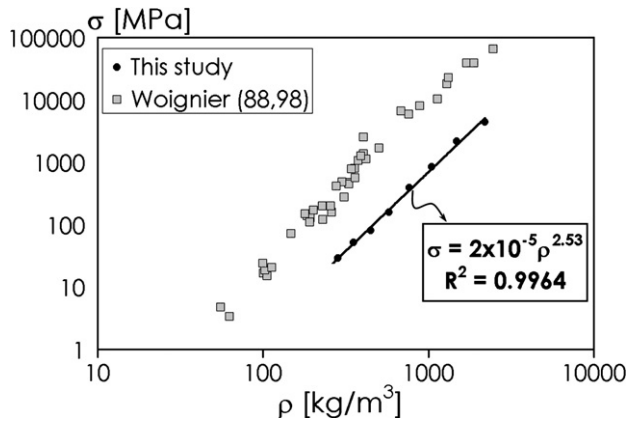

Fig. 6. Strength vs. density for silica aerogels. Woignier [7,9].

Table 2
Exponent for the power law relation between strength and density of porous silica.

Reference	Exponent	Density [g/cm^3]	Observations
This study	2.53 ± 0.15	0.23–2.2	Computer simulation
Woignier et al. [7]	2.6 ± 0.2	0.055–0.5 (approx. values)	Exp. pH neutral, acidic and basic
Woignier et al. [7]	2.3 ± 0.2	0.42–2.2 (approx. values)	Exp. partially densified samples

(density 2.2 g/cm^3) was determined as 63 GPa, which deviates only 12% from the experimental value of 71.9 GPa reported by Muralidharan et al. [24]. Reference [24] summarizes the elastic modulus and the strength that can be obtained using four traditional potentials to model dense SiO_2 systems, namely Soules potential (S-potential), Born–Meyer–Huggins potential (BMH), Feuston–Garofalini potential (FG) and van Beest–Kramer-van Santeen potential (BKS). The minimum deviation between the simulated value and the experimental one is 39% obtained using BKS-potential.

Similarly, the predicted relation between the strength and the density of the samples (Fig. 6) correlates very well with the slope of the experimental data. The main difference is that the magnitude of the strength predicted from the simulations is smaller than the experimental values. The difference is explained based on the values of strength and elastic modulus predicted using other potentials for silica. According to Muralidharan et al. [24] the use of BMH-potential leads to values of strength between 30 and 65 GPa and elastic modulus of 220 GPa, the S-potential leads to values of 24–35 GPa for the strength and 220 GPa for the elastic modulus, for the BKS-potential the strength is obtained between 12 and 22 GPa and an the elastic modulus is 100 GPa, and the FG-potential leads to a strength between 12 and 21 GPa and an elastic modulus of 125 GPa. Those results show that the interatomic potentials are adjusted to reproduced some of the properties of the material; but may not reproduce all of them. The selection of Vashishta's potential for this study is based on its ability to accurately reproduce the structural properties and the elastic modulus of silica. The work presented here shows that, although with limitations, this potential and the method used to prepare the samples can be used to predict how the strength relates to the density for aerogel and xerogel samples.

5. Conclusions

Direct expansion of crystalline samples of β-cristobalite to reach densities between 2.2 g/cm^3 and 0.23 g/cm^3, along with thermal processing, leads to fractal structures which allow to investigate the properties of silica aerogels and xerogels. The geometrical features of the modeled samples are characterized by the fractal dimension, determined from the pair distribution function of the samples as well as from simulated scattering experiments and are found to be in good agreement with computational and experimental data. The fractal region for the samples extends from about 9 to 25 Å, which is inside the fractal range expected for aerogels, 10 to 1000 Å. The size of the samples used for this study do not allow reproducing the macroscopic features of real aerogels, such as pore size distribution and specific surface area; but the results shown here are promising. Work is being done toward using the direct expansion procedure to simulate larger samples and to compare their macroscopic features to those of real aerogels.

Furthermore, the mechanical properties, namely the elastic modulus and strength, of the porous samples are found to scale with density following a power law, which is expected for fractal structures. The exponent of those power law relations are 3.11 ± 0.21 and 2.53 ± 0.15 for elasticity and strength respectively. Those values are in the range determined experimentally. The exponent for the elastic modulus deviates only 3% of the experimental value determined by Woignier et. al. [7] for partially densified aerogels in a similar range of densities than the samples modeled here. For the same samples, the exponent determined here for the relation between strength and density deviates only 10% from the one determined by them.

References

[1] J. Fricke, T. Tillotson, Aerogels: production, characterization and applications, Thin Solid Films 297 (1997) 213–223.
[2] T. Burger, J. Fricke, Aerogels: production, modification and applications, Berichte der Bunsengesellschaft für Physikalische Chemie 102 (11) (1998) 1523–1528.
[3] L.W. Hrubesh, Aerogel applications, Journal of Non-Crystalline Solids 225 (1989) 335–342.
[4] H.D. Gesser, P.C. Goswami, Aerogels and related porous materials, Chemical Reviews 89 (4) (1989) 765–788.
[5] M.N. Rahaman, Ceramic Processing, Taylor & Francis, 2007.
[6] A. Venkateswara Rao, G.M. Pajonk, D. Haranath, P.B. Wagh, Effect of sol–gel processing parameters on optical properties of TMOS silica aerogels, Journal of Materials Synthesis and Processing 6 (1) (1998) 37–48.
[7] T. Woignier, J. Reynes, A. Hafidi Alaoui, I. Beurroies, J. Phalippou, Different kinds of structure in aerogels: relationship with mechanical properties, Journal of Non-Crystalline Solids 241 (1998) 45–52.
[8] T. Woignier, et al., Elastic properties of silica aerogels, Journal of Non-Crystalline Solids 95–96 (1987) 1197–1202.
[9] T. Woignier, J. Phalippou, Mechanical strength of silica aerogels, Journal of Non-Crystalline Solids 100 (1988) 404–408.
[10] J. Groß, J. Fricke, Scaling of elastic properties in highly porous nanostructured aerogels, NanoStructured Materials 6 (1995) 905–908.
[11] A. Rigacci, M.-A. Einarsrud, E. Nilsen, R. Pirard, F. Ehrburger-Dolle, B. Chevalier, Improvement of the silica aerogel strengthening process for scaling-up monolithic tile production, Journal of Non-Crystalline Solids 350 (2004) 196–201.
[12] K. Duer, S. Svendsen, Monolithic aerogel in superinsulating glazings, Solar Energy 63 (4) (1998) 259–267.
[13] A.S. Bahaj, P.A.B. James, M.F. Jentsch, Potential of emerging glazing technologies for highly glazed buildings in hot arid climates, Energy and Buildings 40 (2008) 720–731.
[14] E.M. Lucas, M.S. Doescher, D.M. Ebenstein, K.J. Wahl, D.R. Rolison, Silica aerogels with enhanced durability, 30 nm mean pore size, and improved immersibility in liquids, Journal of Non-Crystalline Solids 350 (2004) 244–252.
[15] R. Vacher, T. Woignier, J. Pelous, Structure and self-similarity of silica aerogels, Physical Review B 37 (11) (1988) 6500–6503.
[16] F. Devreux, J.P. Boilot, F. Chaput, B. Sapoval, NMR determination of the fractal dimension in silica aerogels, Physical Review Letters 65 (5) (1990) 614–617.
[17] T. Woignier, J. Phalippou, R. Vacher, J. Pelous, E. Courtens, Different kinds of fractal structures in silica aerogels, Journal of Non-Crystalline Solids 121 (1990) 198–201.
[18] J. Kieffer, C.A. Angell, Generation of fractal structures by negative pressure rupturing of SiO_2 glass, Journal of Non-Crystalline Solids 106 (1988) 336–342.
[19] A. Nakano, L. Bi, R.K. Kalia, P. Vashishta, Structural correlations in porous silica: molecular dynamics simulation on a parallel computer, Physical Review Letters 71 (1) (1993) 85–88.
[20] T. Campbell, R.K. Kalia, A. Nakano, F. Shimojo, K. Tsuruta, P. Vashishta, Structural correlations and mechanical behavior in nanophase silica glasses, Physical Review Letters 82 (20) (1999) 4018–4021.
[21] P. Vashishta, R.K. Kalia, J.P. Rino, I. Ebbsjö, Interaction potential for SiO_2: a molecular-dynamics study of structural correlations, Physical Review B 15 (1990) 12197–12209.
[22] P. Vashishta, R.K. Kalia, A. Nakano, W. Li, I. Ebbsjö, Molecular dynamics methods and large-scale simulations of amorphous materials, in: M.F. Thorpe, M.I. Mitkova (Eds.), Amorphous Insulators and Semiconductors, NATO ASI Series, 3 High Technology, vol. 23, Kluwer Academic Publishers, 1997, pp. 151–213.
[23] A.C. Wright, The comparison of molecular dynamics simulations with diffraction experiments, Journal of Non-Crystalline Solids 159 (1993) 264–268.
[24] K. Muralidharan, J.H. Simmons, P.A. Deymier, K. Runge, Molecular dynamics studies of brittle fracture in vitreous silica: review and recent progress, Journal of Non-Crystalline Solids 351 (2005) 1532–1542.
[25] M.E. Bachlechner, D. Srivastava, E.T. Owens, J. Schiffbauer, J.T. Anderson, M.R. Burky, S.C. Ducatman, A.M. Gripper, E.J. Guffey, F.S. Ramos, Mechanisms of pit formation at strained crystalline Si(111)/Si_3N_4(0001) interfaces: molecular-dynamics simulations, Physical Review B (Condensed Matter and Materials Physics) 74 (7) (2006) 75327.
[26] A. Chatterjee, R.K. Kalia, C.-K. Loong, A. Nakano, A. Omeltchenko, K. Tsuruta, P. Vashishta, M. Winterer, S. Klein, Sintering, structure and mechanical properties of nanophase SiC: a molecular-dynamics and neutron scattering study, Applied Physics Letters 77 (2000) 1132–1134.
[27] R.W.G. Wyckoff, 2nd ed, Crystal Structures, vol. 1, Intersciense Publishers, 1963.
[28] M.P. Allen, D.J. Tildesley, Computer Simulation of Liquids, Oxford University Press, New York, NY, USA, 1994.
[29] M. Kallala, B. Jullien, B. Cabane, Crossover from gelation to precipitation, Journal de Physique II France 2 (1992) 7–25.
[30] A. Emmerling, J. Fricke, Scaling properties and structure of aerogels, Journal of Sol–Gel Science and Technology 8 (1997) 781–788.
[31] T. Nakayama, K. Yahubo, Dynamical properties of fractal networks: scaling, numerical simulations and physical realizations, Reviews of Modern Physics 66 (2) (1994) 381–443.

[32] V.V. Zosimov, L.M. Lyamshev, Fractals in wave processes, Physics-Uspekhi 38 (4) (1995) 347–484.
[33] J.S. Rivas Murillo, E.J. Barbero, M.E. Bachlechner, D. Cairns, Towards toughening and understanding of silica aerogels — MD simulations, Proceedings of IMECE2008, 2008 ASME International Mechanical Engineering Congress and Exposition, (Oct. 31st–Nov. 6th 2008, Boston, MA, USA), 2008.
[34] K. Mylvaganam, L.C. Zhang, Important issues in a molecular dynamics simulation for characterizing the mechanical properties of carbon nanotubes, Carbon 42 (2004) 2025–2032.
[35] H.J.C. Berendsen, J.P.M. Postma, W.F. van Gunsteren, A. DiNola, J.R. Haak, Molecular dynamics with coupling to an external bath, Journal of Chemical Physics 81 (8) (1984) 3684–3690.
[36] E. Courtens, R. Vacher, Porous silica, in: M.F. Thorpe, M.I. Mitkova (Eds.), Amorphous Insulators and Semiconductors, NATO ASI Series, 3 High Technology, vol. 23, Kluwer Academic Publishers, 1997, pp. 255–288.